Journal of Physics:
Conference Series

PAPER • OPEN ACCESS

Parametric Investigation of Wing Geometric Characteristics for Enhancing UAV Endurance

To cite this article: Shehab Hassouna and Ashraf Mohamed Kamal 2025 *J. Phys.: Conf. Ser.* **3070** 012008

Parametric Investigation of Wing Geometric Characteristics for Enhancing UAV Endurance

Shehab Hassouna[1*] **and Ashraf Mohamed Kamal**[2]

[1]M.Sc Student, Aircraft Mechanics Department, Military Technical College, Cairo, Egypt.
[2]Assistant Professor,Aircraft Mechanics Department, Military Technical College, Cairo, Egypt.

[*]E-mail: shehabhassouna57@gmail.com

Abstract. Improving endurance in airplane design is important for specific types such as in medium altitude long endurance (MALE) unmanned aerial vehicle (UAV). Achieving this objective requires obtaining the best wing geometric characteristics that maximize the relevant aerodynamic parameters without compromising the overall performance. In this study, a parametric investigation is performed using the USAF DATCOM mid-fidelity aerodynamic tool to examine the effect of varying taper ratio, aspect ratio, and sweep angle on a baseline wing configuration of a case study MALE UAV. The analysis begins with evaluating the aerodynamic characteristics of the selected wing, followed by a systematic variation of the geometric parameters, while maintaining the original airfoil and wing area. First, thirty different wing configurations are generated by varying the taper and aspect ratios, from which the most aerodynamically efficient configuration is selected for further evaluation by varying the sweep angle. The results indicate that increasing aspect ratio has the most significant effect on improving endurance, followed by taper ratio, whereas increasing sweep angle reduces endurance.

Keywords
Flight Endurance, Flight Range, MALE UAV, USAF DATCOM

List of Symbols

AR = aspect ratio
b_1 = inner panel span (m)
C_D = drag coefficient
C_L = lift coefficient
C_{L_α} = lift curve slope (1/rad)
C_r = root chord (m)
c_P = power-specific fuel consumption (kg/(W · s))
R = range (m)
V = velocity (m/s)
W_i = initial weight (kg)
α = angle of attack (rad)
η_p = propeller efficiency
Λ_{In} = inner panel sweep angle (°)
ρ = air density (kg/m^3)
b = span (m)
b_2 = outer panel span (m)
C_{D_o} = zero-lift drag coefficient
$C_{L_{max}}$ = maximum lift coefficient
C_{m_o} = zero angle pitching moment coefficient
C_t = tip chord (m)
E = endurance (s)
S = wing area (m^2)
W = aircraft weight (kg)
W_f = final weight (kg)
α_{stall} = stall angle of attack (rad)
λ = taper ratio
Λ_{Out} = outer panel sweep angle (°)

1. Introduction

Medium altitude long endurance (MALE) UAVs have numerous functions; some of them are long endurance of up to 40 hours, for example (IAI Heron, Chengdu Wing Loong-3, and Yabhon United 40 UAVs), high payload capacities, for example (Aksungur UAV can carry up to 750 kg), reconnaissance/advanced surveillance for hazardous areas, and versatile mission profiles for example target acquisition and precision strikes.

In 2002, Altman [1] created a program to identify the conceptual design and sizing variables that most influenced the design of a propeller-driven High Altitude Long Endurance Unmanned Aerial Vehicle (HALE UAV). He also performed a sensitivity analysis of the endurance performance, which was isolated into three main categories; the first one is operational environment and includes cruise altitude and cruise velocity/cruise lift coefficient, the second one is aircraft Wing Geometry which includes taper ratio, aspect ratio and Wing Profile and the last one is engine configuration. He used the vortex lattice method in his analysis; the results show that the endurance is most influenced by cruise altitude, aspect ratio,taper ratio,cruise lift coefficient and airfoil selection.

In 2014, Zakaria and Ahmed [2] discussed the results of a parametric study on a flying wing SUAV, focusing on the design of wing extensions in a low subsonic free stream. Two design parameters of the wing extensions are discussed, namely, the span and the taper ratio. The study aims to vary these two parameters and assess their influence on the endurance of the wing. They used USAF DATCOM to obtain the results. It was found that the aerodynamic performance was improved by adding the extensions, and the relative span was found to have a dominant role in this respect.

In 2017, Panagiotou and Yakinthos [3] used a CFD-aided parametric study of the Blended Wing Body (BWB) concept at low subsonic speeds. The parametric study was conducted to examine the BWB concept under low subsonic, incompressible flow conditions and to show the effect of the key design variables on the efficiency of the platform. They used (Vortex Lattice Method) [4] as a low-fidelity method and CFD with Ansys CFX as a high-fidelity method. They varied the wing sweep angle and wing aspect ratio. They found that a wing sweep of 0° was the most efficient at a medium angle of attack range and low subsonic operational speeds, which is the operational regime of most MALE surveillance UAVs, the subject of our case study. The variation of aspect ratio study concludes that the lift curve slope of the BWB increases with increasing aspect ratio, whereas the slope of the traditional concept remains practically unaffected.

In 2018, Valencia, Hidalgo, and Rodríguez [5] developed a versatile and adaptable method to assess the aerodynamic performance of UAVs based on parametric and semi-empirical models in the open domain. They applied the classical Lifting Line Theory [6] and the VLM (Vortex Lattice Method) [4] and semi-empirical relations to estimate the drag developed for civil aviation. Then, CFD simulations over the wing were conducted using the commercial software Ansys Fluent to calibrate the model. From the parametric analysis, it was found that aerodynamic performance can be affected in different ways, such as by the operating conditions and geometrical parameters. The study of wing aerodynamic performance comprised the assessment of four geometrical parameters: aspect ratio, taper ratio, setting angle, and twist angle. They found parametric and semi-empirical tools can be embraced as alternatives during the conceptual design of unmanned aircraft, obtaining results with acceptable accuracy.

The objective of this research is to conduct a parametric study on the wing of the selected case study MALE UAV to enhance endurance primarily without compromising other performance parameters (e.g., range, rate of climb, stall speed, etc.) and range secondarily by varying dimensionless parameters such as taper ratio and aspect ratio.

Then selecting the best configuration from different wing planform shapes that achieve the goal. The sweep angle of chosen configurations will then be varied for further investigation. Thirty different configurations are developed, and their aerodynamic characteristics are estimated using the powerful aerodynamic tool USAF DATCOM.

2. MALE UAV Case Study

Figure 1 shows a 3D CAD drawing of the selected MALE UAV , where its important specifications are presented in table 1 :

Journal of Physics: Conference Series **3070** (2025) 012008 doi:10.1088/1742-6596/3070/1/012008

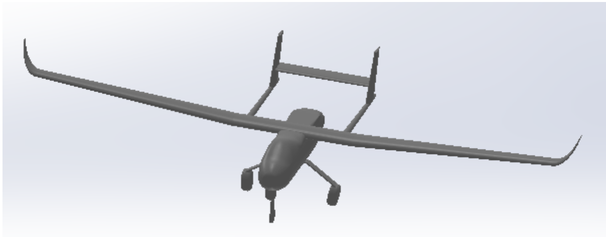

Figure 1. The 3D CAD drawing of the selected case-study UAV

Table 1. Main specifications of base study of the MALE UAV

Parameter	**Specification**
Max level airspeed	$\geq$ 180 km/hr
Cruise speed	120–140 km/hr
Min speed	110 km/hr
Max climb rate	5 m/s
Practical ceiling	5 km
Endurance (50 kg payload)	10 hr
Max take-off weight	340 kg
Mission payload	50 kg
Max fuel weight	95–100 kg
Engine	HS700GB
Propeller	Two-blade wooden fix-pitch (diameter 0.9 m)
Propeller design advance ratio	0.52
Propeller design efficiency	0.65

The baseline configuration of the wing planform for the case study MALE UAV is shown in figure 2. Additionally, table 2 summarizes the main characteristics of the wing. The airfoils are specially designed as given in figure 3 so there is an aerodynamic twist in the wing and their aerodynamic characteristics will be in figure 4.

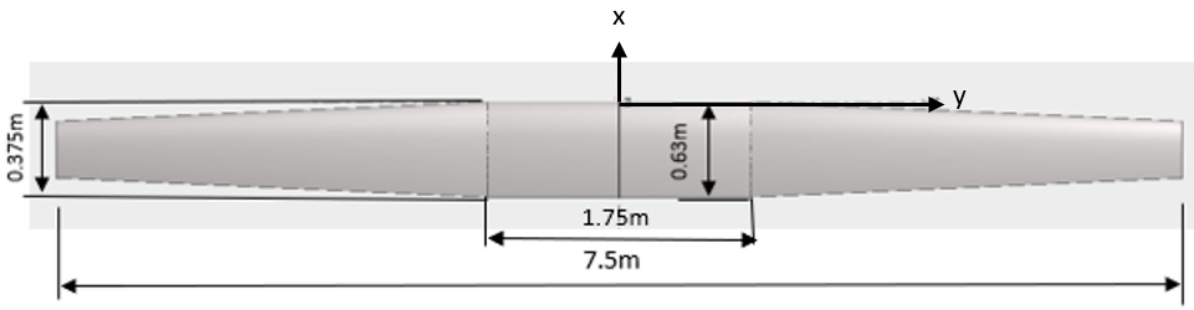

Figure 2. MALE UAV wing planform

Table 2. Wing geometric characteristics

Parameter	Value	Parameter	Value
b	7.5 m	S	4 m^2
MAC	0.548 m	C_r	0.63 m
λ	0.587	b_1	1.75 m
C_t	0.375 m	AR	14
Dihedral angle of Outer Panel	4°	b_2	5.75 m

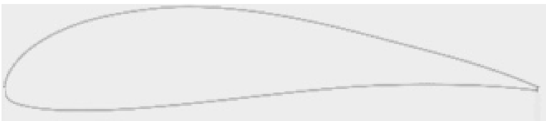

(a) Root airfoil for the wing case-study

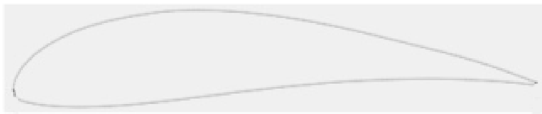

(b) Tip airfoil for the Wing case-study

Figure 3. Root and tip airfoils for the wing case-study

The aerodynamic characteristics of the baseline UAV wing configuration are calculated using USAF DATCOM at a cruise speed of 36 m/s and an altitude of 3 km and presented in comparison with the root and tip airfoils' aerodynamics as shown in figure 4. On the other hand, the aerodynamic performance parameters corresponding to maximum range and endurance are calculated and presented in figure 5.

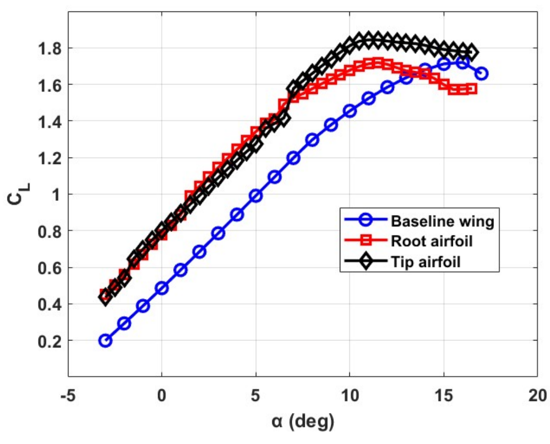

(a) Lift curve for baseline wing, root airfoil and tip airfoil

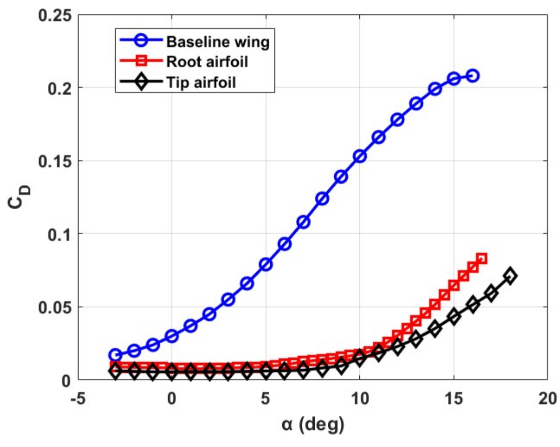

(b) Drag curve for baseline wing, root airfoil and tip airfoil

Figure 4. Lift and drag curves for baseline Wing, root airfoil and tip airfoil

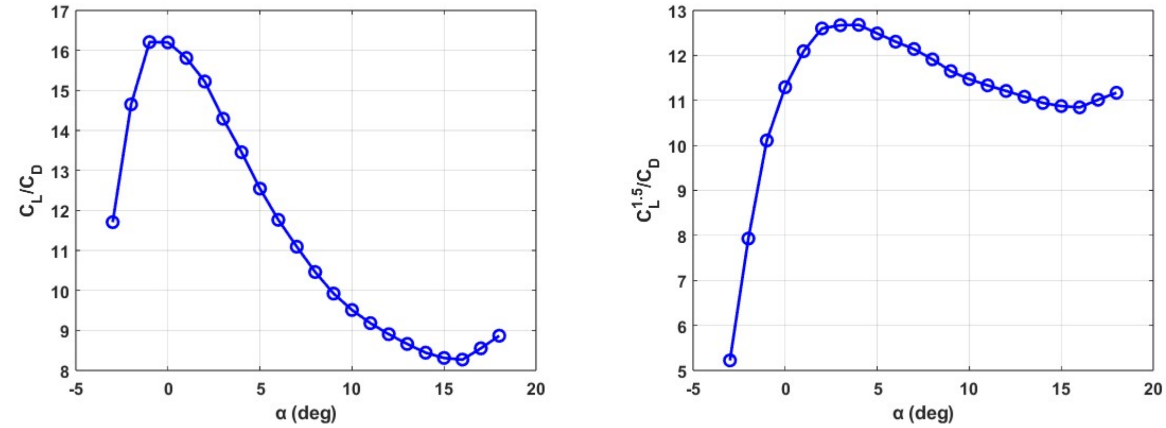

(a) Aerodynamic parameter corresponding to maximum range for wing case Study

(b) Aerodynamic parameter corresponding to maximum endurance for wing case study

Figure 5. Aerodynamic parameters corresponding to maximum range and endurance for wing case study at a cruise speed of 36 m/s and an altitude of 3 km

Based on figures 4 and 5 the most important values of wing aerodynamic performance parameters and their corresponding angle of attack that significantly affect the performance of the case-study UAV are summarized in table 3:

Table 3. Aerodynamic performance parameters

Parameter	Value	Corresponding (α)
$C_{L_{\max}}$	1.72	16°
Maximum Range $\left(\frac{C_L}{C_D}\right)$	16.2	0°
Maximum Endurance $\left(\frac{C_L^{1.5}}{C_D}\right)$	12.68	4°

3. Parametric Study of the Wing

In order to select the wing geometric parameters that affect the endurance and range of the case-study UAV, the Breguet endurance and range equations mentioned in [4] as per equations 1 and 2. Based on the equations, the parameters that are affected by changing the wing geometry are considered variables, while others are considered constant as given in table 4:

$$E = \frac{\eta_p}{c_P} \frac{C_L}{C_D} \sqrt{\frac{\rho\, S\, C_L}{2W}} \ln\left(\frac{W_i}{W_f}\right) \tag{1}$$

$$R = \frac{\eta_p}{c_P} \frac{C_L}{C_D} \ln\left(\frac{W_i}{W_f}\right) \tag{2}$$

Table 4. Fixed and varied parameters for endurance and range equations

Parameter	Value
η_p	Fixed
c_P	Fixed
ρ	Fixed
S	Fixed
W	Fixed
C_L	Variable
C_D	Variable

The study is carried out at an altitude of 3 km for a fixed cruising velocity of 36 m/s. The wing will be divided into two panels: inner and outer panels. The span of the inner panel will be kept constant at 1.75 m to maintain the tail booms at their original position. The chord of the inner panel will be assigned as a variable ranging from 0.4 m to 0.63 m to obtain six chord configurations with a step of 0.05 m while the last step will be 0.03 m. This will result in a reduction in the inner panel area, which will be redistributed to the outer panel area to keep the total area of the wing constant. For each of the six chord configurations above, the taper ratio will be varied from 0.5 to 0.9 with a step of 0.1. This will consequently change the aspect ratio. In total, 30 configurations are obtained as shown in table 5. The methodology adopted in this research to investigate the effect of wing geometric characteristics on the aerodynamic performance parameter is summarized in the flowchart shown in figure 6:

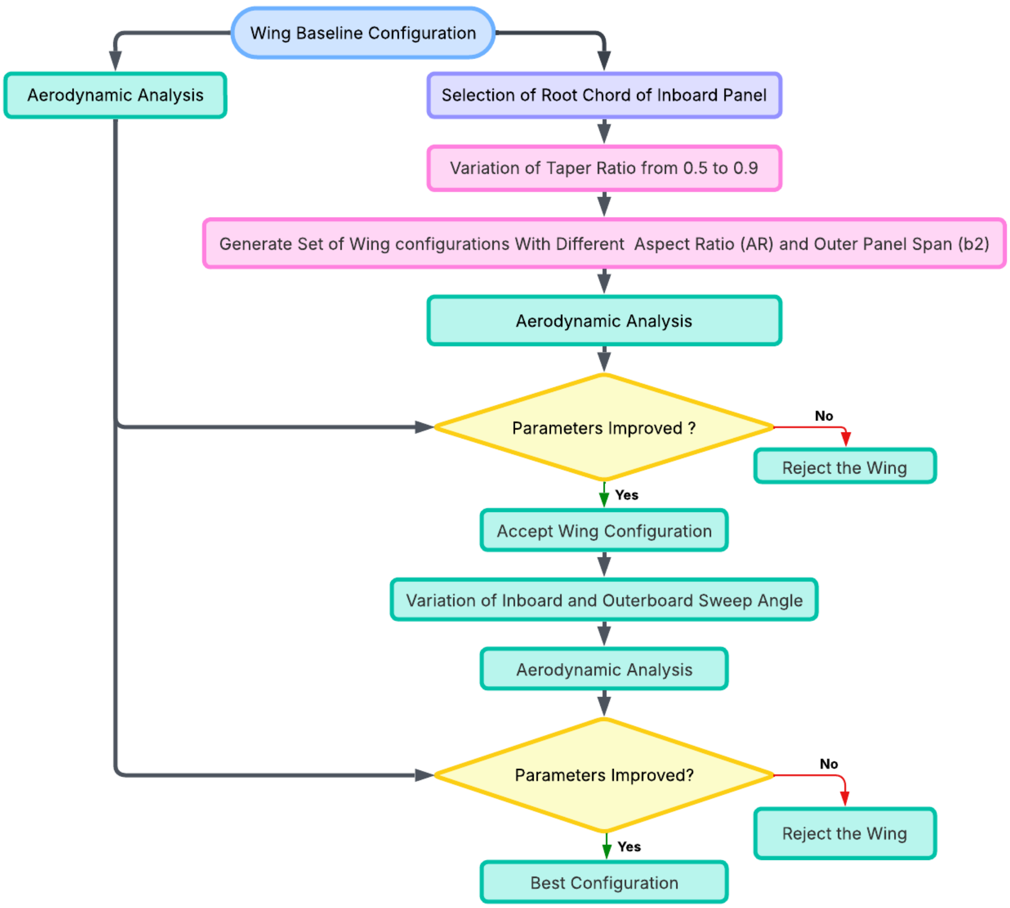

Figure 6. Flowchart For Case Study

After choosing the best configuration to further enhance endurance and range, the sweep angle of the inner and outer panels will be parametrically varied. For each of the following Λ_{In}: 0°, 5°, 10°, and 15°, there will be four corresponding Λ_{Out}: 0°, 5°, 10°, and 15° listed respectively. This results in 16 additional configurations to investigate. Table 5 lists the different taper and aspect ratios for the thirty configurations.

Table 5. Aspect ratio, taper ratio, and outer panel span for the generated 30 cases

Case No.	**Root Chord,** C_r	**Taper Ratio,** λ	**Aspect Ratio, AR**	**Outer Panel Span,** b_2 (m)
First Case	$C_r = 0.4\ m$	0.5	40.6	12.8
		0.6	36.4	12.1
		0.7	32.8	11.5
		0.8	29.8	10.9
		0.9	27.2	10.4
Second Case	$C_r = 0.45\ m$	0.5	31.8	11.3
		0.6	28.5	10.7
		0.7	25.8	10.1
		0.8	23.4	9.7
		0.9	21.5	9.3
Third Case	$C_r = 0.5\ m$	0.5	25.4	10.1
		0.6	22.9	9.6
		0.7	20.7	9.1
		0.8	18.8	8.7
		0.9	17.3	8.3
Fourth Case	$C_r = 0.55\ m$	0.5	20.8	9.1
		0.6	18.7	8.7
		0.7	17.0	8.2
		0.8	15.6	7.9
		0.9	14.3	7.6
Fifth Case	$C_r = 0.6\ m$	0.5	17.3	8.3
		0.6	15.6	7.9
		0.7	14.2	7.5
		0.8	13.0	7.2
		0.9	11.9	6.9
Sixth Case	$C_r = 0.63\ m$	0.5	15.5	7.9
		0.6	14.1	7.5
		0.7	12.8	7.2
		0.8	11.8	6.9
		0.9	10.9	6.6
Baseline Case	$C_r = 0.63\ m$	0.59	14.2	7.5

4. Results and Discussions

Based on the different cases shown in table 5, the USAF DIGITAL DATCOM is used to obtain aerodynamic characteristics of each configuration. Figures 7 , 8, 9,10 and 11 show the variation of the lift curve, the aerodynamic parameter for maximum endurance coefficient ($\frac{C_L^{1.5}}{C_D}$), and range coefficient ($\frac{C_L}{C_D}$) for each taper ratio. There are 7 cases of the different dimensions of the root chord in table 5. All aerodynamic characteristics are extracted, which include (C_{D_o}, $\frac{C_L^{1.5}}{C_D}$, C_{M_o}, $\frac{C_L}{C_D}$, $C_{L_{\max}}$, α_{stall}, and $C_{L\alpha}$), and assigning weights to them based on the objectives of this study as given in table 6.

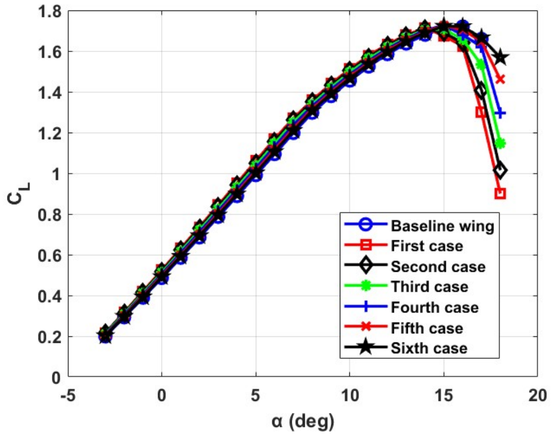

(a) Lift Curve for $\lambda = 0.5$

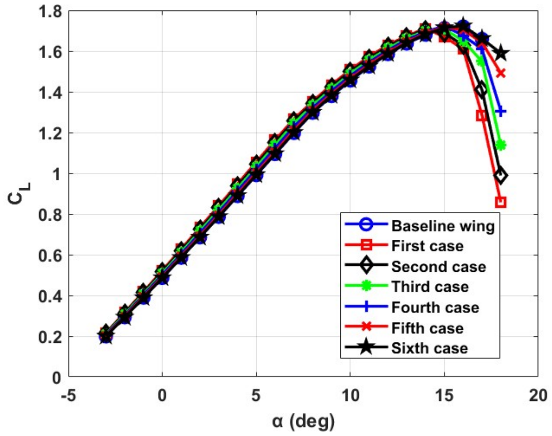

(b) Lift Curve for $\lambda = 0.6$

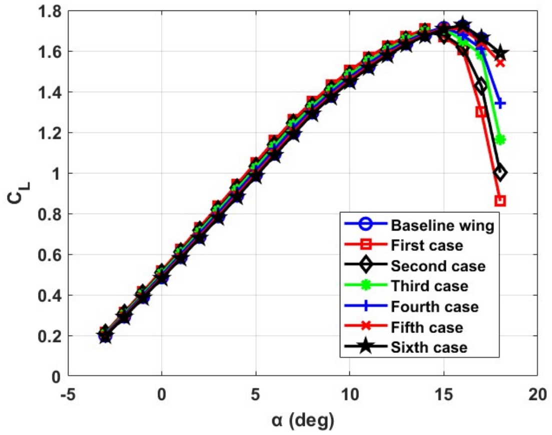

(c) Lift Curve for $\lambda = 0.7$

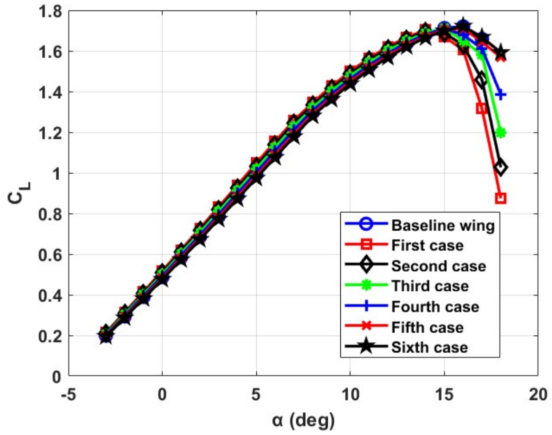

(d) Lift Curve for $\lambda = 0.8$

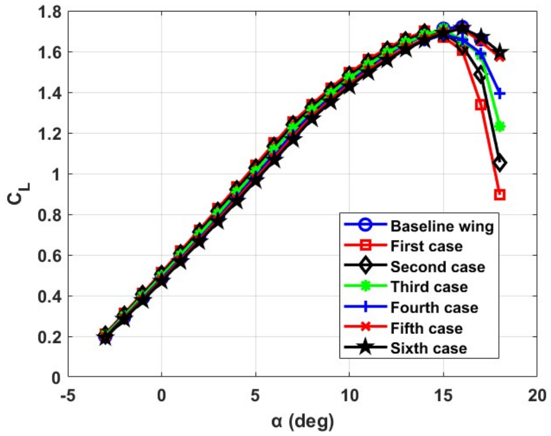

(e) Lift Curve for $\lambda = 0.9$

Figure 7. Lift curves for different cases with different λ

From figure 7, by increasing the aspect ratio (span) and decreasing the taper ratio, α_{stall} decreases from 16° to 15°, resulting in a steeper stall behavior (and vice versa).

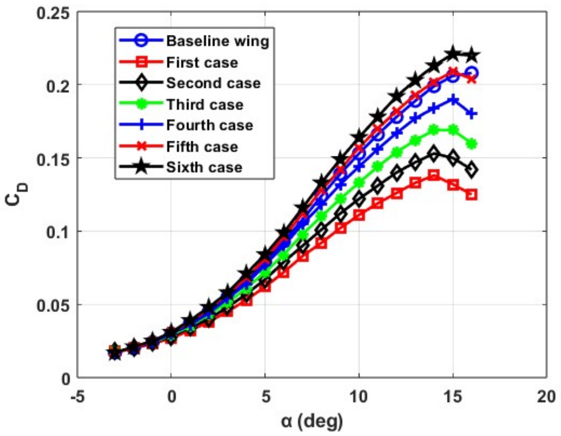

(a) Drag Curve for $\lambda = 0.5$

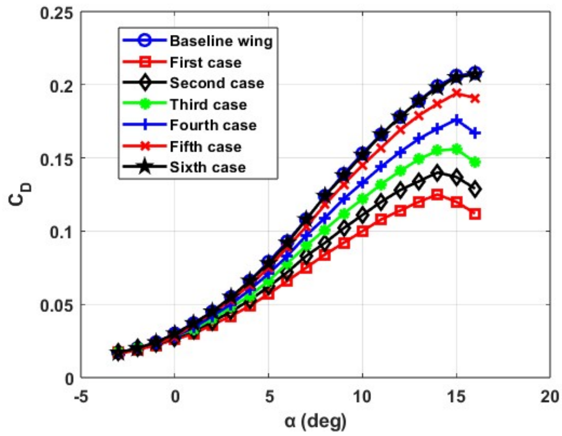

(b) Drag Curve for $\lambda = 0.6$

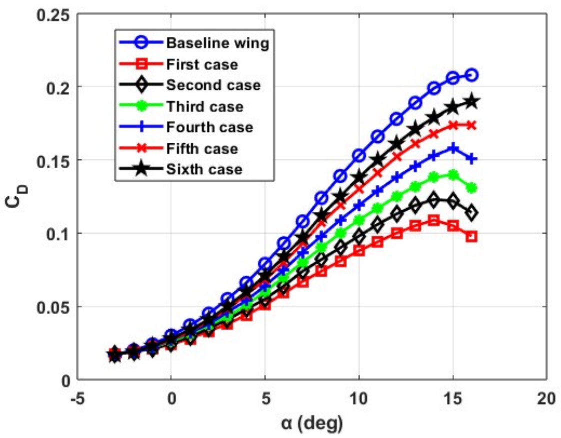

(c) Drag Curve for $\lambda = 0.7$

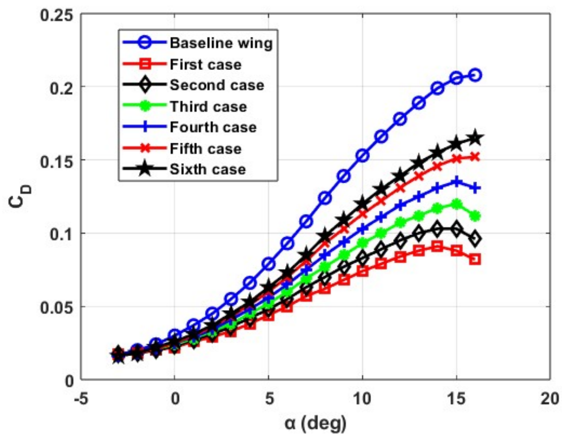

(d) Drag Curve for $\lambda = 0.8$

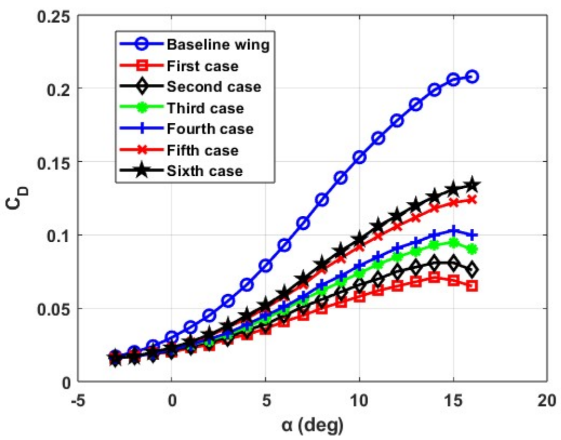

(e) Drag Curve for $\lambda = 0.9$

Figure 8. Drag curves for different cases with different λ

From figure 8, by increasing the aspect ratio (span) and the taper ratio, there is a significant decrease in the drag, approximately 33.34% for the first case with $C_r = 0.4m$ and $\lambda = 0.9$.

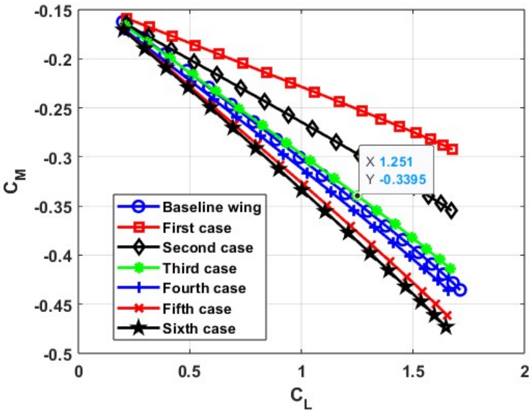

(a) Pitching moment Curve for $\lambda = 0.5$

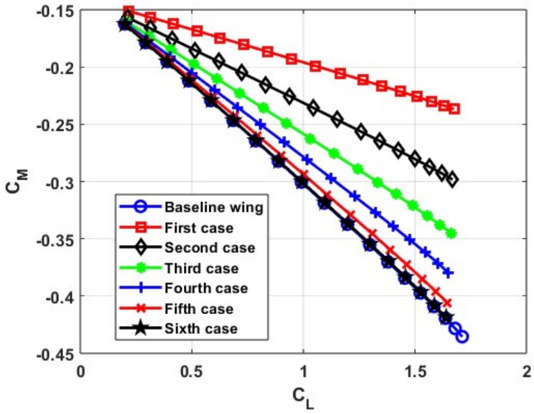

(b) Pitching moment Curve for $\lambda = 0.6$

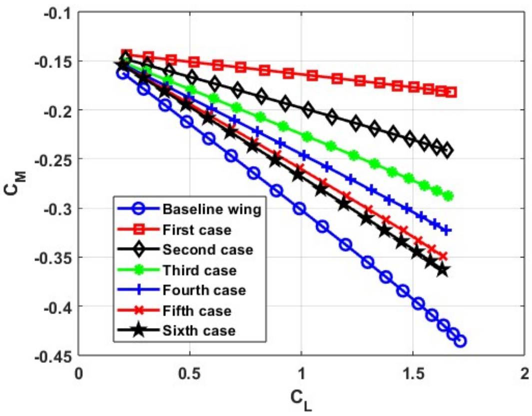

(c) Pitching moment Curve for $\lambda = 0.7$

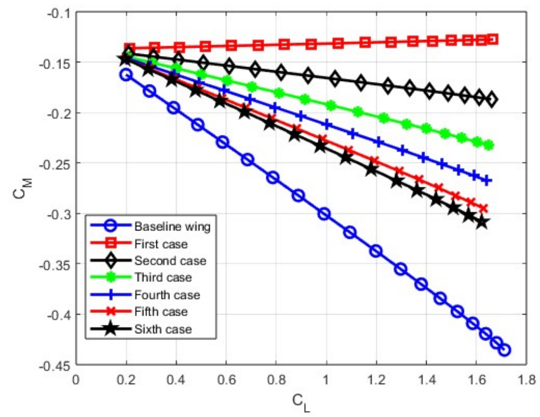

(d) Pitching moment Curve for $\lambda = 0.8$

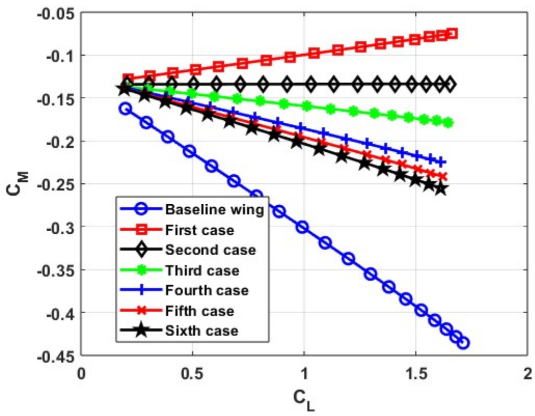

(e) Pitching moment Curve for $\lambda = 0.9$

Figure 9. Pitching moment curves for different cases with different λ

Figure 9 shows that increasing both the aspect and taper ratios has a positive impact on the reduction of the absolute value of the zero-lift pitching moment coefficient. This, in turn, contributes to a decrease in the required horizontal tail volume ratio coefficient (i.e., reduces horizontal tail area and/or tail arm).

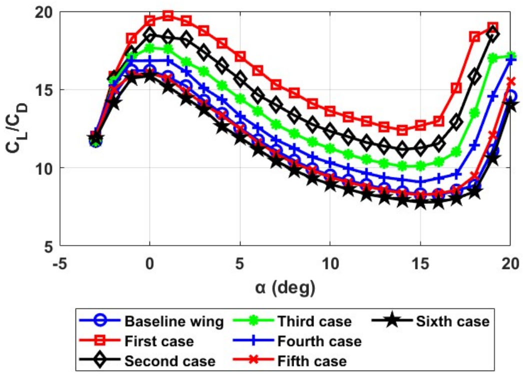

(a) Aerodynamic parameter corresponding to maximum range for $\lambda = 0.5$

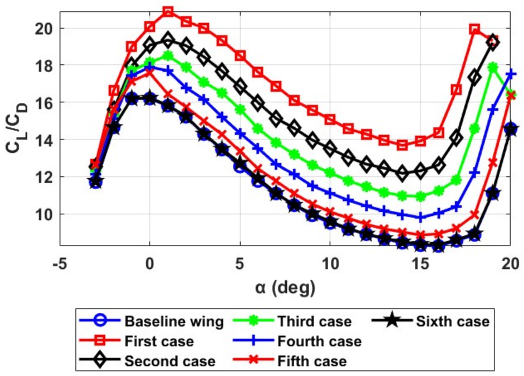

(b) Aerodynamic parameter corresponding to maximum range for $\lambda = 0.6$

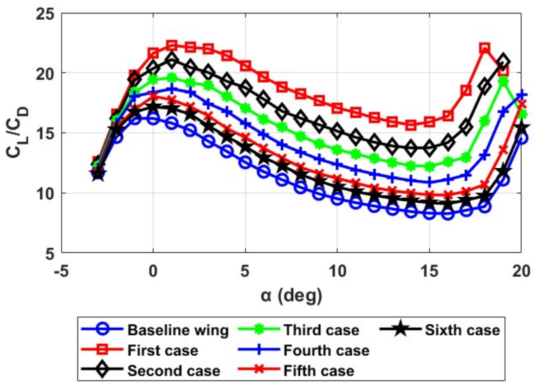

(c) Aerodynamic parameter corresponding to maximum range for $\lambda = 0.7$

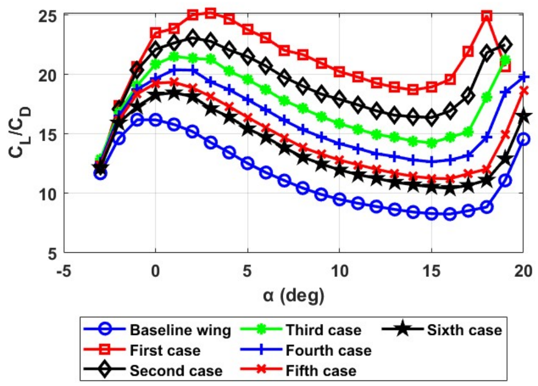

(d) Aerodynamic parameter corresponding to maximum range for $\lambda = 0.8$

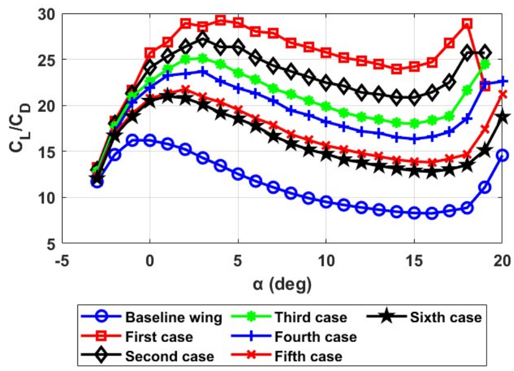

(e) Aerodynamic parameter corresponding to maximum range for $\lambda = 0.9$

Figure 10. Aerodynamic parameter corresponding to maximum range for different cases with different λ

From figure 10, by increasing AR and λ, there is a significant increase in the aerodynamic parameter for maximum range, approximately 80.39% for the first case with $C_r = 0.4m$ and $\lambda = 0.9$.

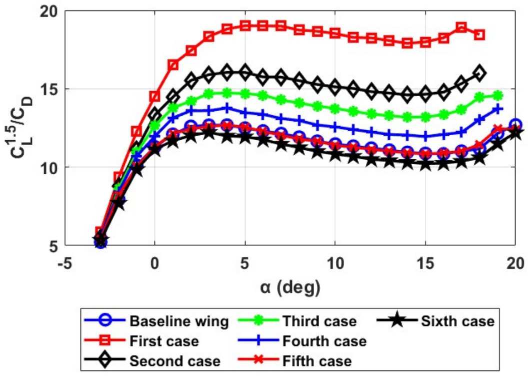

(a) Aerodynamic parameter corresponding to maximum endurance for $\lambda = 0.5$

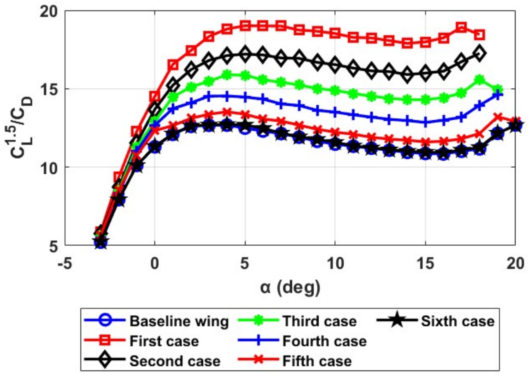

(b) Aerodynamic parameter corresponding to maximum endurance for $\lambda = 0.6$

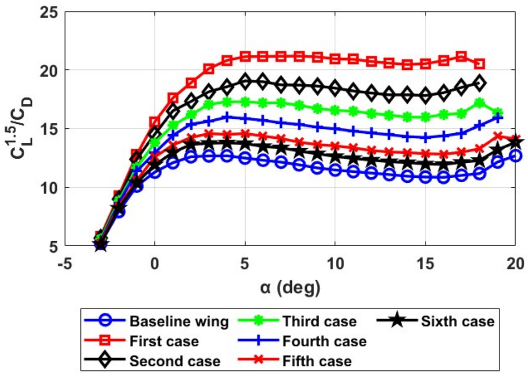

(c) Aerodynamic parameter corresponding to maximum endurance for $\lambda = 0.7$

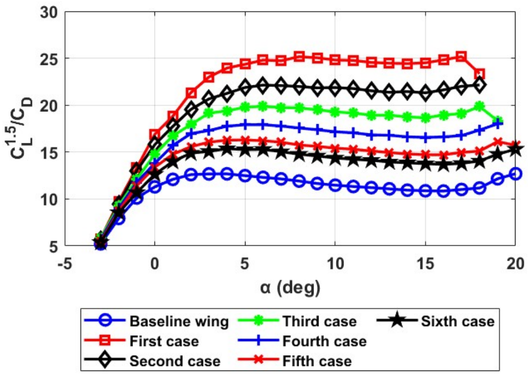

(d) Aerodynamic parameter corresponding to maximum endurance for $\lambda = 0.8$

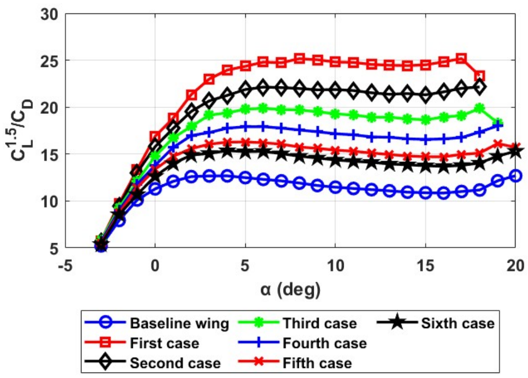

(e) Aerodynamic parameter corresponding to maximum endurance for $\lambda = 0.9$

Figure 11. Aerodynamic parameter corresponding to maximum endurance for different cases with different λ

From figure 11, by increasing AR and λ, there is an increase in the aerodynamic parameter for maximum endurance, approximately 149.3% for the first case with $C_r = 0.4$ and taper ratio = 0.9..

Table 6. Weight of parameters

Parameter	$\frac{C_L^{1.5}}{C_D}$	$\frac{C_L}{C_D}$	C_{Do}	$C_{L_{\max}}$	C_{Mo}	$C_{L\alpha}$	α_{stall}
Weight	35%	20%	15%	10%	10%	5%	5%

The weighting factors shown in table 6 were determined in line with our design objectives. Aerodynamic parameters that directly impact maximum endurance and range—specifically, ($\frac{C_L^{1.5}}{C_D}$) for endurance and ($\frac{C_L}{C_D}$) for range and are assigned the highest weights to boost overall efficiency. Next, reducing drag by minimizing the zero-lift drag coefficient, (C_{D_o}), is prioritized. A high maximum lift coefficient, ($C_{L_{\max}}$), is given importance to reduce the lift-off speed and consequently reduce the takeoff and landing distance. Additionally, a lower moment coefficient at zero lift, (C_{M_o}), is targeted to enable a smaller empennage area. Furthermore, a steep lift curve (indicating a large change in lift for a small change in α) and a low stall angle, (α_{stall}), are both emphasized to further enhance cruise and takeoff performance. These selections reflect a balanced approach to optimizing both cruise efficiency and short-field performance without compromising overall other performance parameters.

The configuration with the highest score is selected from the thirty evaluated configurations. In particular, the configuration with $C_r = 0.4\,\text{m}$ and $\lambda = 0.9$ achieved the highest score of 59.7%. The best wing geometric parameters are presented in table 7 and the corresponding aerodynamic parameters in table 8.

Table 7. Wing geometric characteristics of the best configuration

Parameter	**Value**
b	10.434 m
C_t	0.36 m
AR	27.218
C_r	0.4 m
λ	0.9
MAC	0.384 m

Table 8. Values of parameters of the best configuration

Parameter	$\frac{C_L^{1.5}}{C_D}$	$\frac{C_L}{C_D}$	C_{Do}	$C_{L_{\max}}$	C_{Mo}	$C_{L\alpha}$	α_{stall}
Value	31.60448	29.21875	0.02	1.699	-0.117	0.1056	14

The best wing configuration is then taken, and another study is conducted to investigate the influence of sweep angle changes on this wing from quarter chord sweep angle. The results are presented in figures 12 , 13, 14, 15 and 16.

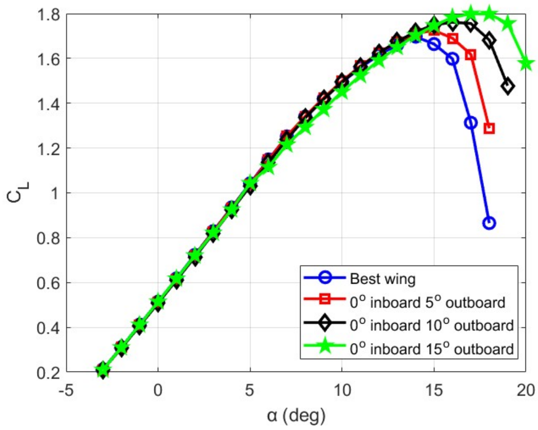

(a) Lift curve for best wing configuration with $\Lambda_{In} = 0^o$ and variable Λ_{Out}

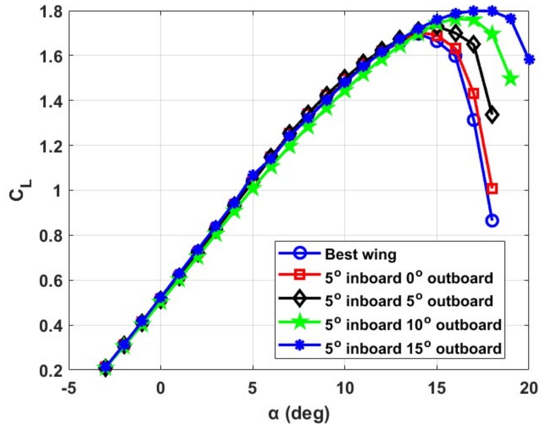

(b) Lift curve for best wing configuration with $\Lambda_{In} = 5^o$ and variable Λ_{Out}

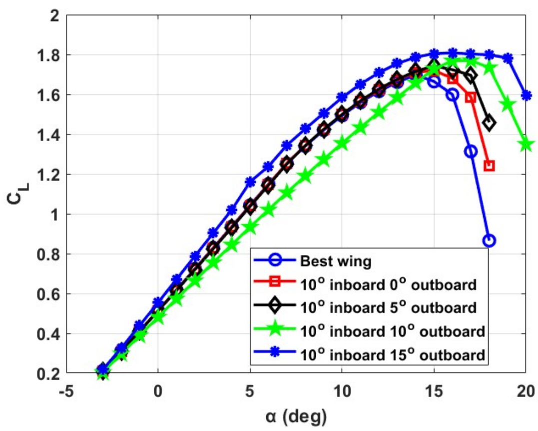

(c) Lift curve for best wing configuration with $\Lambda_{In} = 10^o$ and variable Λ_{Out}

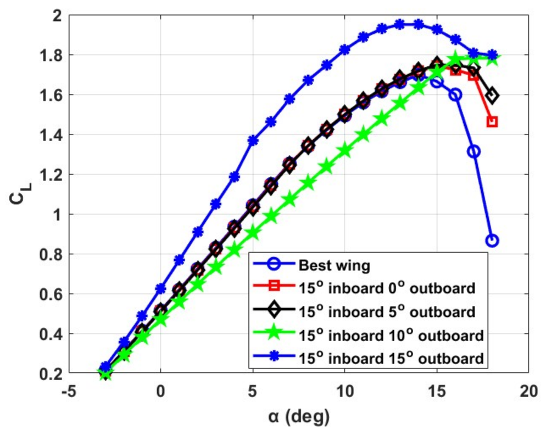

(d) Lift curve for best wing configuration with $\Lambda_{In} = 15^o$ and variable Λ_{Out}

Figure 12. Lift curve for best wing configuration with variable Λ_{In} and variable Λ_{Out}

By increasing both Λ_{In} and Λ_{Out}. For example, for the configuration with $\Lambda_{In}= 15^o$ and $\Lambda_{Out}= 15^o$, there is a significant increase of about 13.37% approximately in $C_{L_{\max}}$ compared with the best wing configuration that was obtained from AR and λ variations, while α_{stall} remains as it is 14^o, but with a gentle stall behavior.

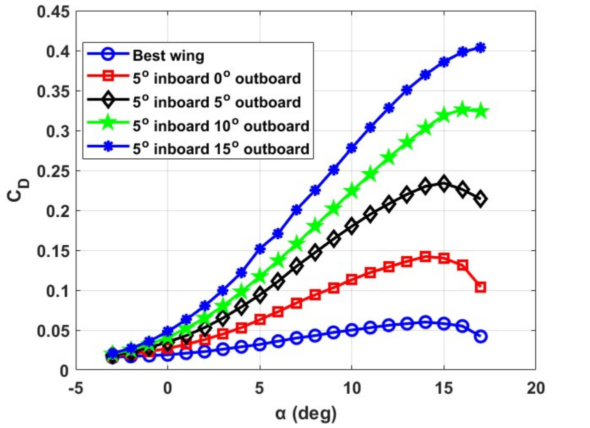

(a) Drag curve for best wing and best wing configuration with $\Lambda_{In} = 0^o$ and variable Λ_{Out}

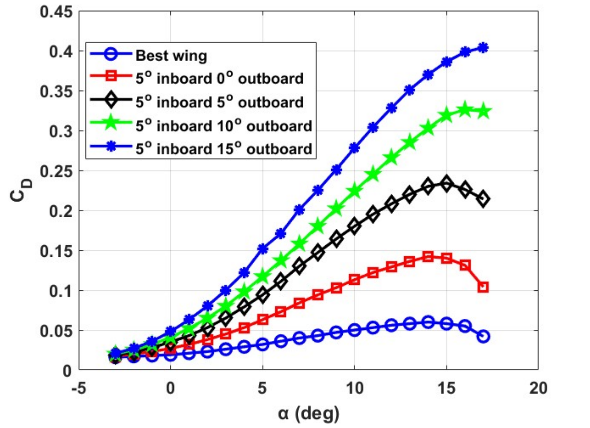

(b) Drag curve for best wing and best wing configuration with $\Lambda_{In} = 5^o$ and variable Λ_{Out}

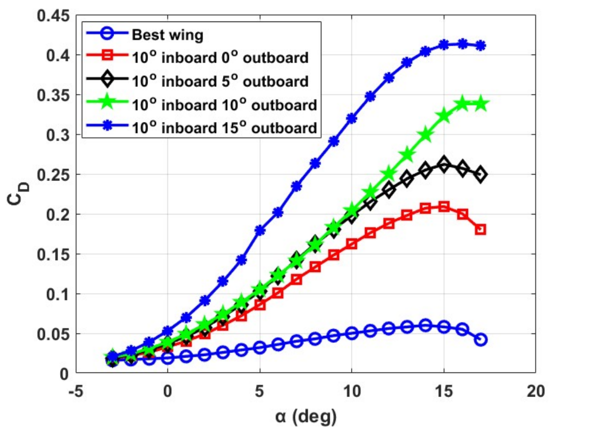

(c) Drag curve for best wing and best wing configuration with $\Lambda_{In} = 10^o$ and variable Λ_{Out}

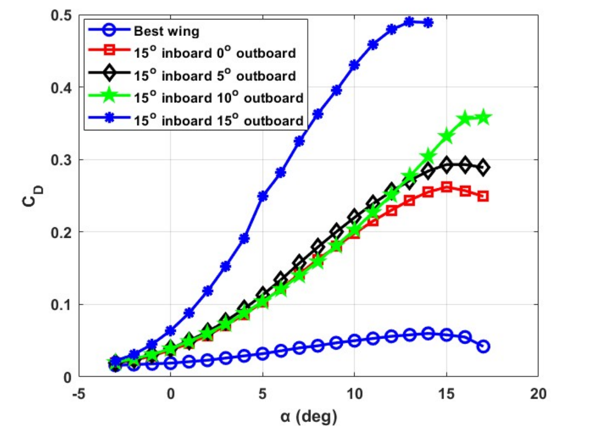

(d) Drag curve for best wing and best wing configuration with $\Lambda_{In} = 15^o$ and variable Λ_{Out}

Figure 13. Drag curves for best wing configuration with variable Λ_{In} and variable Λ_{Out}

By increasing both Λ_{In} and Λ_{Out} , there is a significant increase for C_{D_o}. For example, for the configuration with $\Lambda_{In}= 0^o$ and $\Lambda_{Out}= 10^o$, there is an increase in C_{D_o} of about 116% compared with the best wing configuration that was obtained from AR and λ variations, while for the configuration with $\Lambda_{In}= 15^o$ and $\Lambda_{Out}= 15^o$, C_{D_o} increases about 205% compared with the best wing configuration.

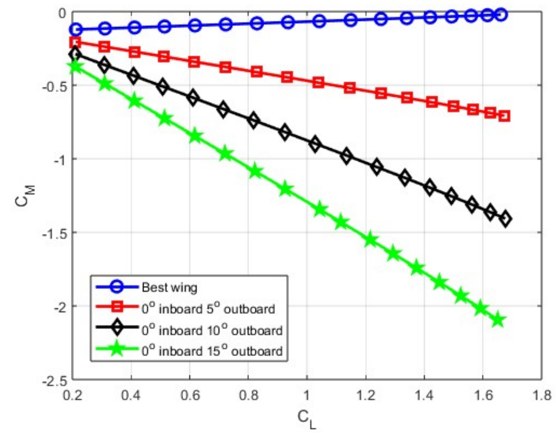

(a) Pitching moment curve for best wing and best wing configuration with $\Lambda_{In} = 0^o$ and variable Λ_{Out}

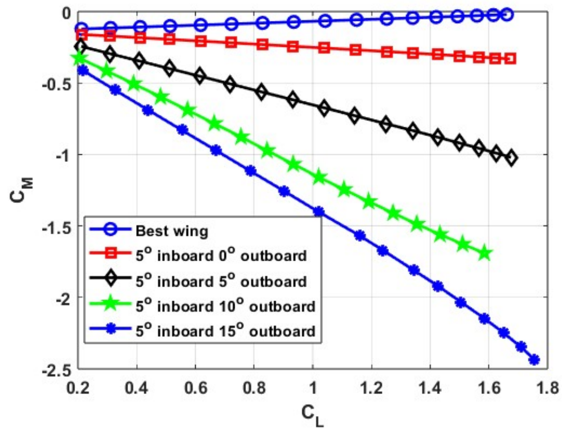

(b) Pitching moment curve for best wing and best wing configuration with $\Lambda_{In} = 5^o$ and variable Λ_{Out}

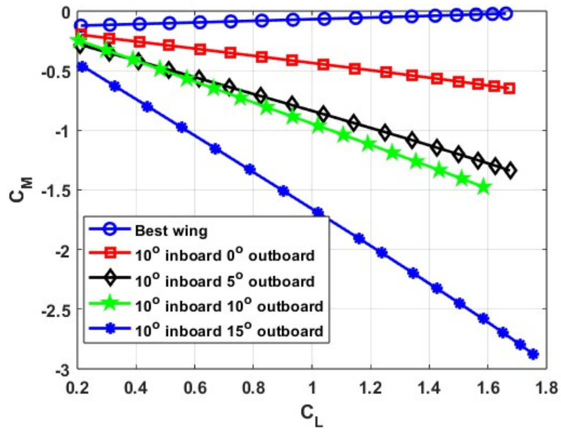

(c) Pitching moment curve for best wing and best wing configuration with $\Lambda_{In} = 10^o$ and variable Λ_{Out}

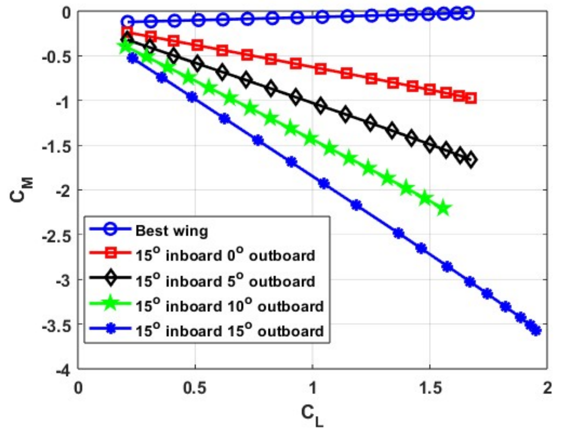

(d) Pitching moment curve for best wing and best wing configuration with $\Lambda_{In} = 15^o$ and variable Λ_{Out}

Figure 14. Pitching moment curves for best wing configuration with variable Λ_{In} and variable Λ_{Out}

As illustrated in figure 14, changing both the inboard and outboard sweep angles negatively impacts the reduction of the zero-lift pitching moment coefficient when compared to the best configuration obtained from variations in aspect and taper ratios. This suggests that changing the sweep angles necessitates either an increase in the horizontal tail area or an extension of the tail arm, which negatively affects the performance of the UAV.

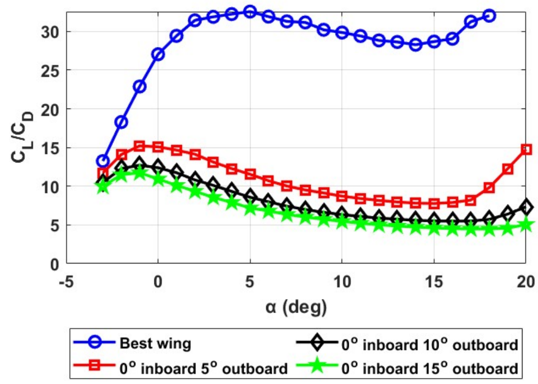

(a) Aerodynamic parameter corresponding to maximum range for best wing configuration with $\Lambda_{In} = 0^o$ and variable Λ_{Out}

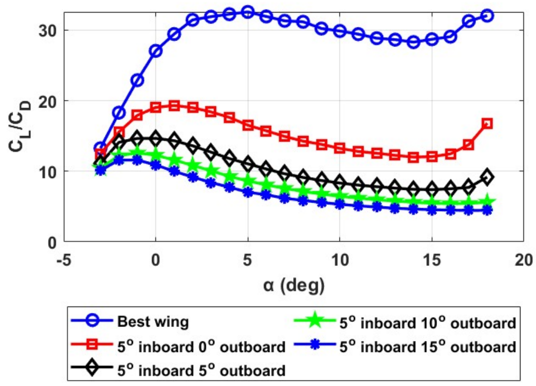

(b) Aerodynamic parameter corresponding to maximum range for and best wing configuration with $\Lambda_{In} = 5^o$ and variable Λ_{Out}

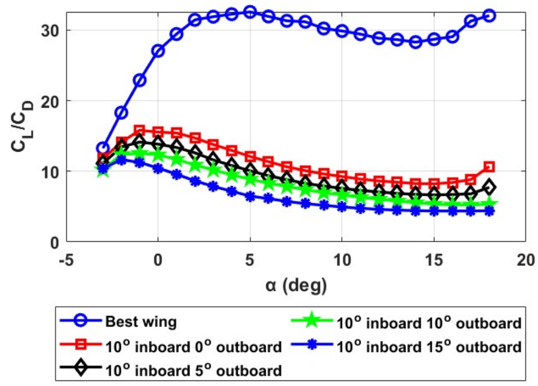

(c) Aerodynamic parameter corresponding to maximum range for best wing configuration with $\Lambda_{In} = 10^o$ and variable Λ_{Out}

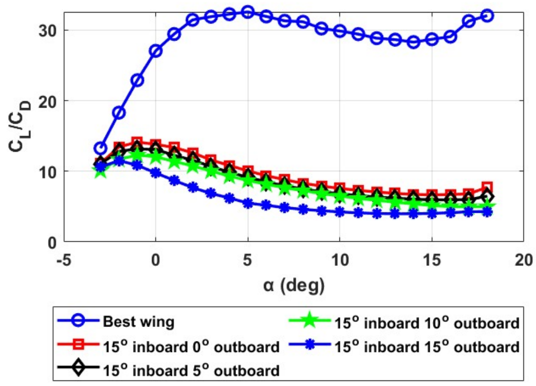

(d) Aerodynamic parameter corresponding to maximum range for best wing configuration with $\Lambda_{In} = 15^o$ and variable Λ_{Out}

Figure 15. Aerodynamic parameter corresponding to maximum range for best wing configuration with variable Λ_{In} and variable Λ_{Out}

From figure 12, there is an increase in (C_L) but the increase in (C_{D_o}) dominates as shown in figure 13. For example, the configuration with Λ_{In}= 15^o and Λ_{Out}= 15^o, so the value of $((C_L/C_D)_{max})$ decreases approximately by 199%.

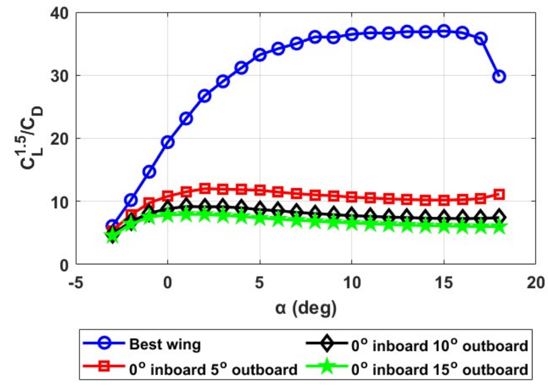

(a) Aerodynamic parameter corresponding to maximum endurance and best wing configuration with $\Lambda_{In} = 0^o$ and variable Λ_{Out}

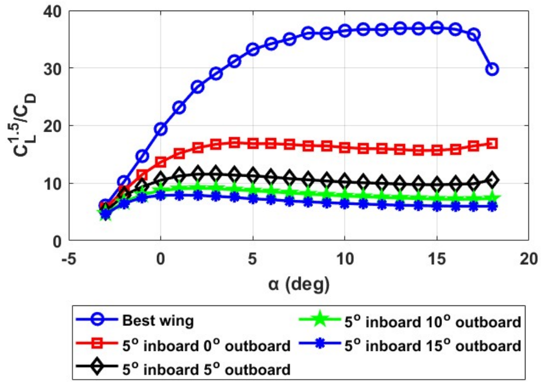

(b) Aerodynamic parameter corresponding to maximum endurance and best wing configuration with $\Lambda_{In} = 5^o$ and variable Λ_{Out}

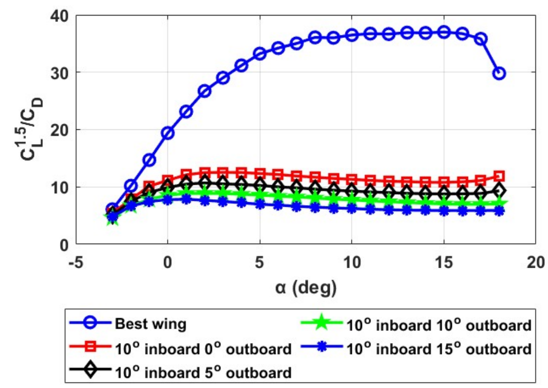

(c) Aerodynamic parameter corresponding to maximum endurance and best wing configuration with $\Lambda_{In} = 10^o$ and variable Λ_{Out}

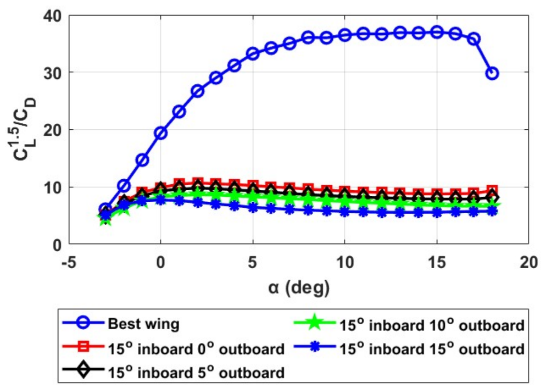

(d) Aerodynamic parameter corresponding to maximum endurance best wing configuration with $\Lambda_{In} = 15^o$ and variable Λ_{Out}

Figure 16. Aerodynamic parameter corresponding to maximum endurance best wing configuration with variable Λ_{In} and variable Λ_{Out}

Similarly, figure 16 shows that the increase of C_D dominates the increase of C_L. For the configuration with $\Lambda_{In}= 15^o$ and $\Lambda_{Out}= 15^o$, the value of $((C_L^{1.5}/C_D)_{max})$ decreases approximately by 310%. Therefore, varying sweep angle increases lift and α_{stall} while decreasing endurance and range parameters.

The aerodynamic parameters change for the best wing configuration aiming at endurance and range is shown in the following table 9:

Table 9. Comparison of aerodynamic parameters between baseline and best wing configurations

Parameter	Baseline Configuration	Best Configuration	Change (%)
$(\frac{C_L^{1.5}}{C_D})_{max}$	12.68	31.61	↑ 149.3%
$(\frac{C_L}{C_D})_{max}$	16.2	29.22	↑ 80.37%
C_{D_o}	0.03	0.02	↓ 33.34%
$C_{L_{\max}}$	1.72	1.69	↓ 1.2%
C_{M_o}	-0.212	-0.117	↑ 44.8%
C_{L_α}	0.101	0.106	↑ 4.55%
α_{stall}	16	14	↓ 12.5%

5. Conclusion and Future work

In this research, a parametric study is conducted to enhance MALE UAV endurance by varying the main wing geometric characteristics. The results indicate that increasing the aspect ratio significantly improves the endurance as it increases the relevant aerodynamic efficiency. The second parameter identified to enhance the endurance is the increase in the taper ratio of the outboard panel. Conversely, increasing the sweep angle negatively affects the lift-to-drag ratio. Although the results suggest increasing the aspect ratio, such an increase introduces structural and weight constraints which are outside the scope of the current study and are carefully addressed in a separate research.

Thus, future work should include a multidisciplinary optimization methodology that integrates aerodynamic, structure, weight and performance. Additionally, a higher fidelity aerodynamic tool (e.g., CFD) should be used to refine and validate the aerodynamic data and their consequent conclusions obtained in this study.

6. Acknowledgments

The authors would like to express their sincere gratitude to Associate Professor M. Y. Zakaria for his valuable academic contributions to this research. His insightful feedback, critical discussions, and guidance throughout the course of this work have been instrumental in shaping the direction and depth of the study.

References

[1] A. Altman, "A parametric study on design variables effecting hale uav aircraft design for a conventional configuration," 05 2002.

[2] M. Zakaria and M. Ahmed, "Parametric study on wing tip extensions for suav," *Proceedings of the 1st World Congress on Unmanned Systems Engineering*, 01 2014.

[3] P. Panagiotou and K. Yakinthos, "Parametric aerodynamic study of blended-wing-body platforms at low subsonic speeds for uav applications," 06 2017.

[4] J. D. Anderson, *Fundamentals of Aerodynamics*, 6th ed. Columbus, USA: McGraw-Hill, 2017.

[5] E. A. Valencia, V. Hidalgo, and D. Rodriguez, *Parametric modelling for aerodynamic assessment of a fixed wing UAV implemented for Site Specific Management.* [Online]. Available: https://arc.aiaa.org/doi/abs/10.2514/6.2018-0988

[6] I. H. Abbott and A. E. Von Doenhoff, *Theory of wing sections: including a summary of airfoil data.* Courier Corporation, 2012.